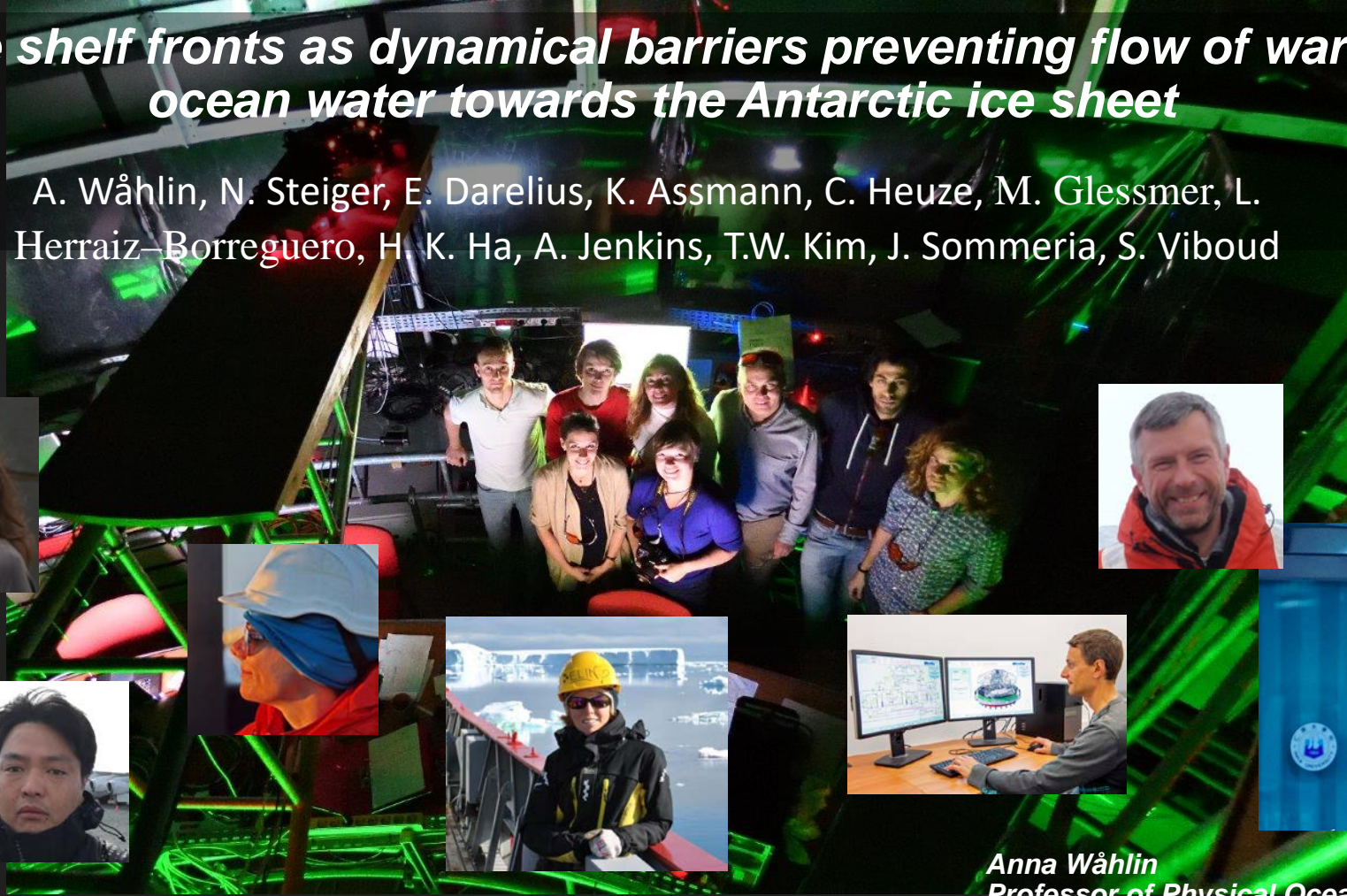


Ice shelf fronts as dynamical barriers preventing flow of warm ocean water towards the Antarctic ice sheet

A. Wåhlin, N. Steiger, E. Darelius, K. Assmann, C. Heuze, M. Glessmer, L. Herraiz-Borreguero, H. K. Ha, A. Jenkins, T.W. Kim, J. Sommeria, S. Viboud



Anna Wåhlin
Professor of Physical Oceanography
University of Gothenburg, Sweden

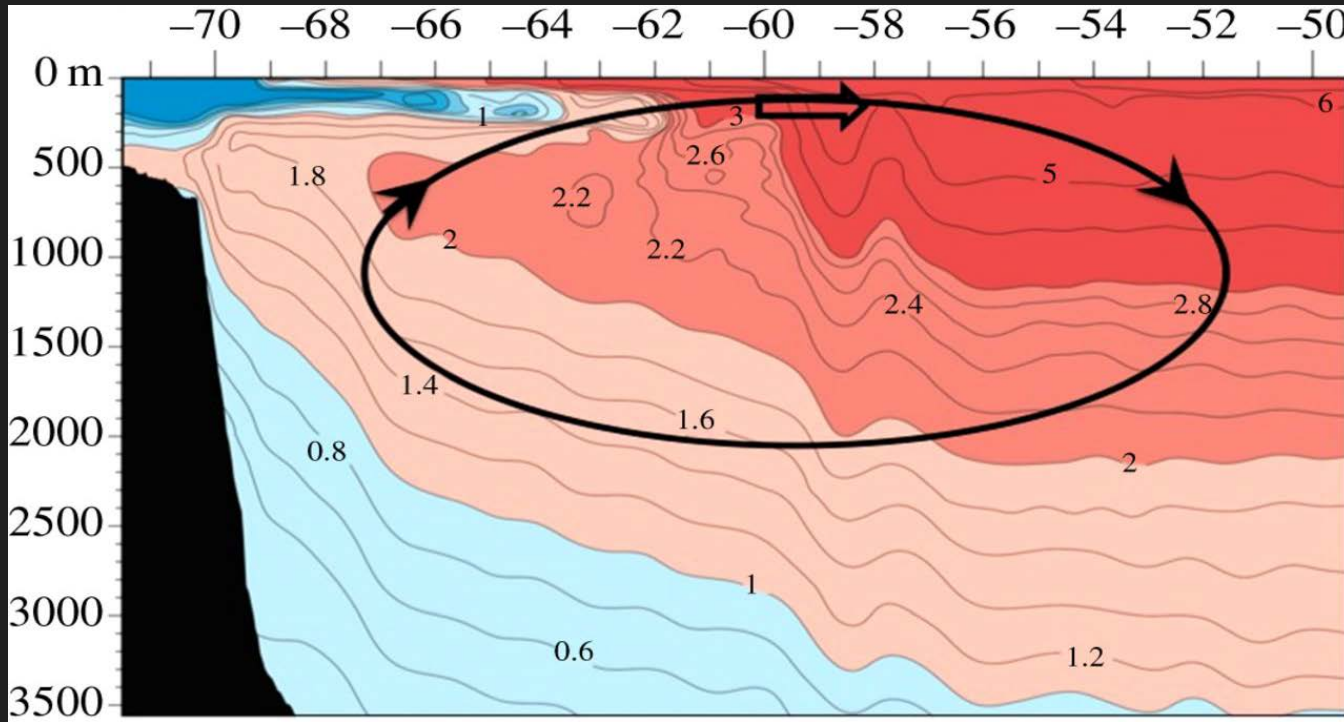
Results published in this paper:

Wåhlin, A. K., Steiger, N., E. Darelius, K. M. Assmann, M. S. Glessmer, H. K. Ha, L. Herraiz-Borreguero, C. Heuzé, A. Jenkins, T. W. Kim, A. K. Mazur, J. Sommeria & S. Viboud, 2020. Ice front blocking of ocean heat transport to an Antarctic ice shelf, *Nature*, 578, 568-571. <https://doi.org/10.1038/s41586-020-2014-5>

Free access to pdf here: <https://rdcu.be/b2dCD>

Circumpolar deep water: A pool of warm water residing between 1500-500 m depth outside the Antarctic continental shelf

Heat available to melt ice in this pool, S of 60°S is $E = 1.2 \cdot 10^{20} \text{ kJ}$



$$E = \iint_A \int_D^0 C_P \rho (T - T_F) dz dA$$

$C_P = 2.97 \text{ kJ/K/kg}$ is the specific heat capacity

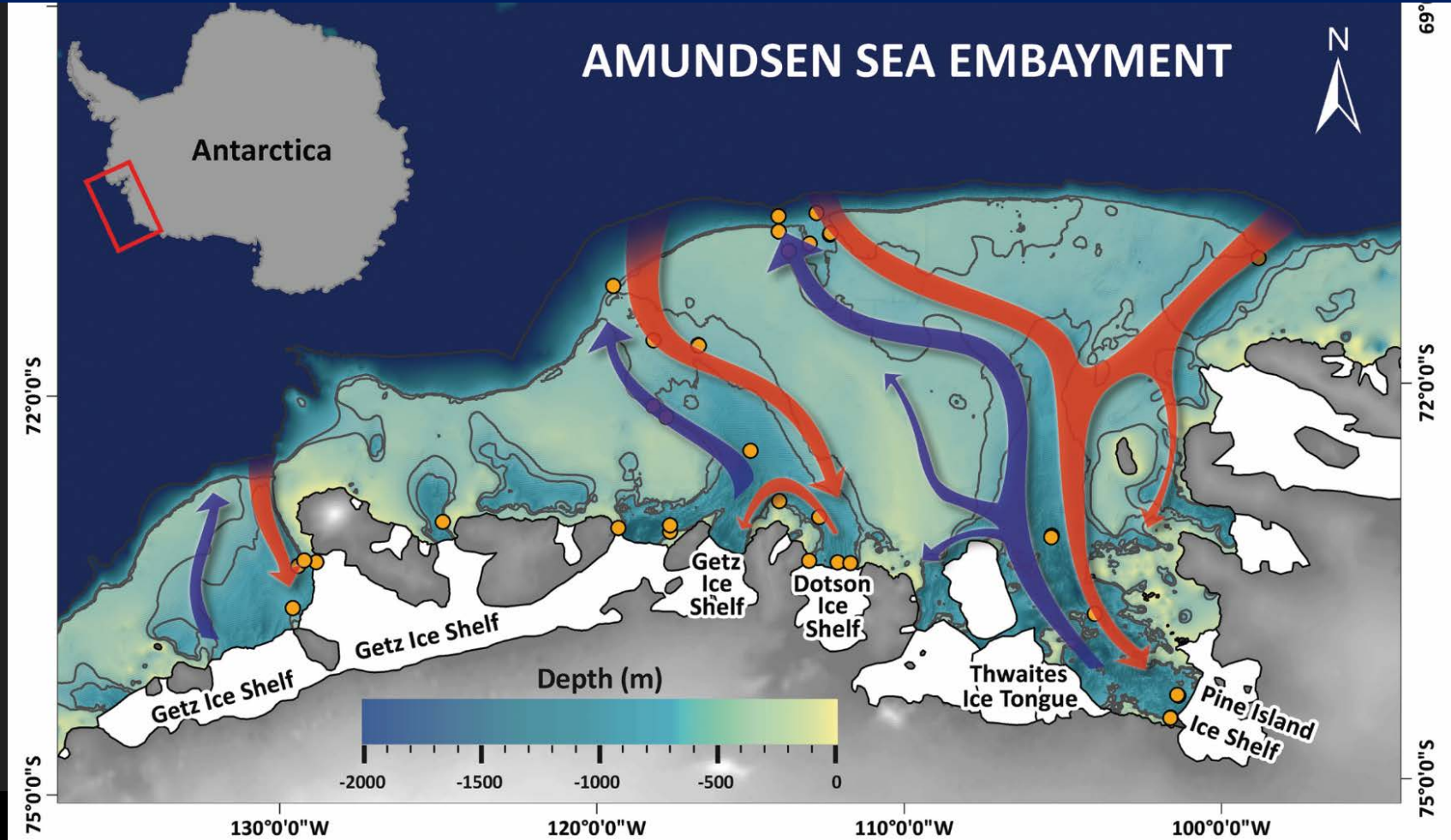
ρ is the density

T is temperature

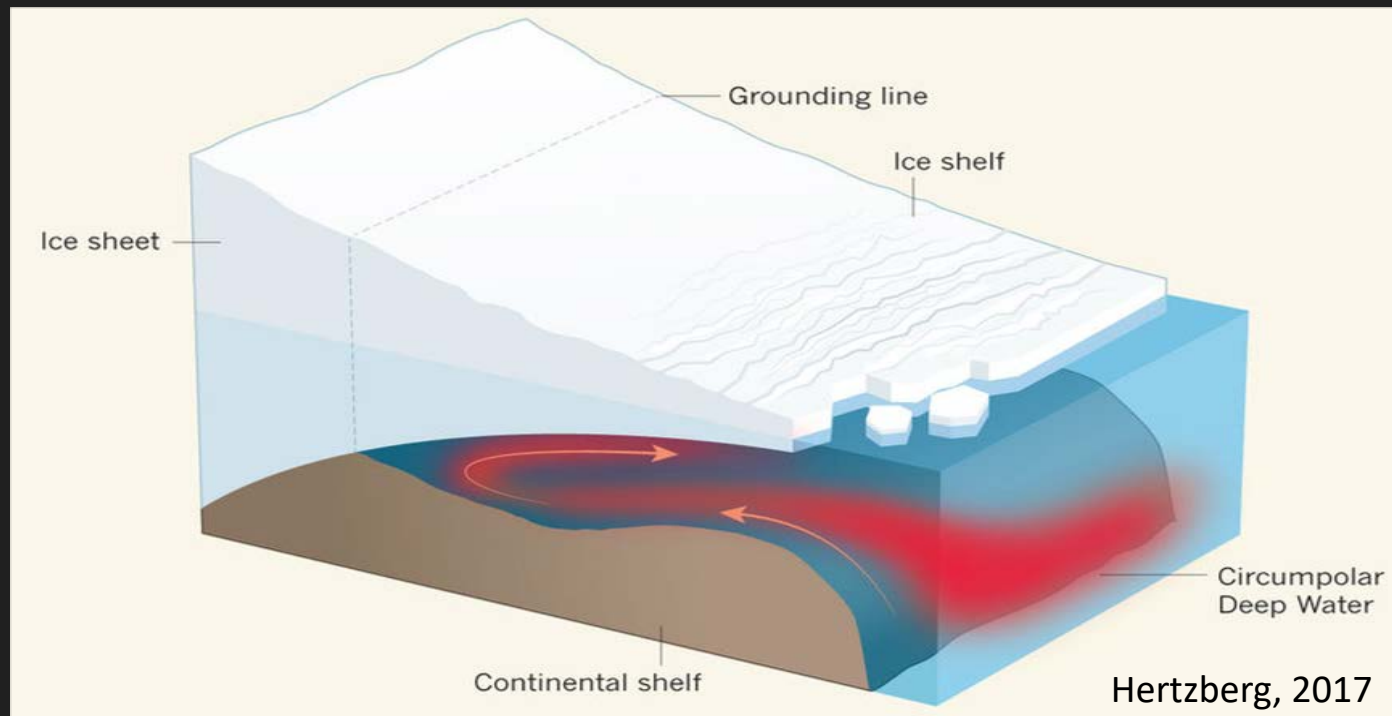
T_F is freezing point

This is equivalent to the entire atmosphere S of 60°S being 400°C

Warm water flows towards the glaciers in deep troughs on the continental shelf



...but: How much can enter underneath the ice shelf and access the grounding line..?
Shoreward ocean heat flux at the shelf break typically exceeds the melt rates of glaciers^{1,2}
Are there constraints and upper limits on transport set by fluid dynamics...?



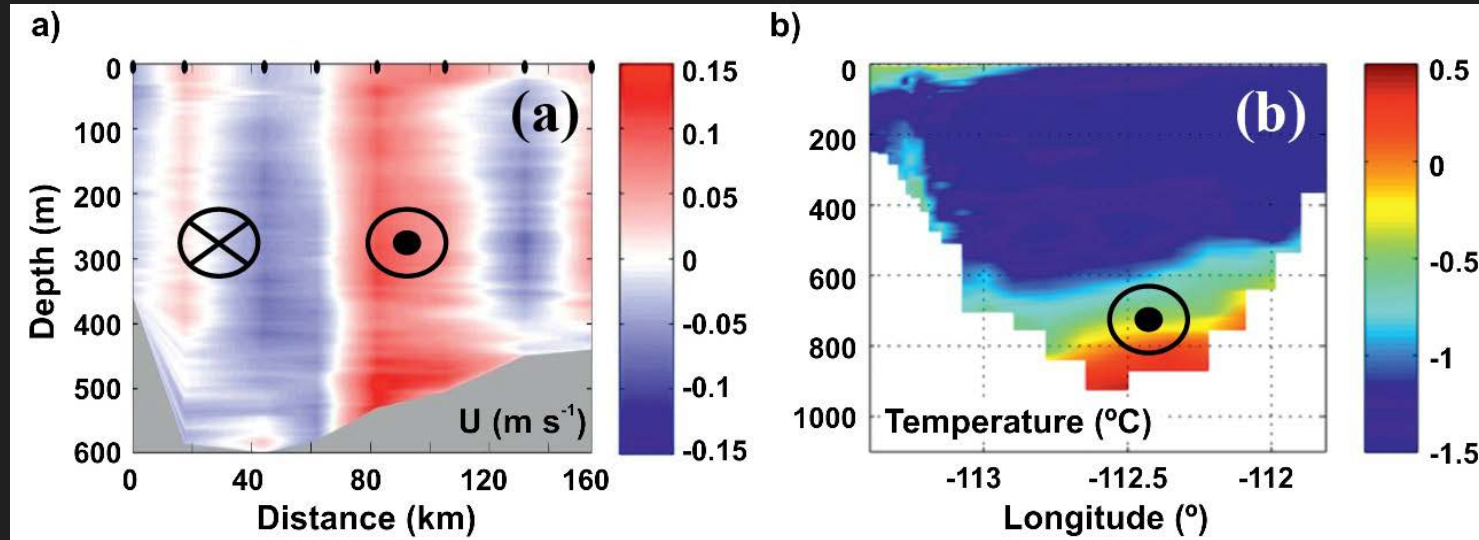
1) Pritchard, H. D. et al. Antarctic ice-sheet loss driven by basal melting of ice shelves. *Nature* 484, 502–505 (2012).

2) Palóczy, A., Gille, S. T. & Mcclean, J. L. Oceanic Heat Delivery to the Antarctic Continental Shelf : Large-Scale , Low-Frequency Variability. *J. Geophys. Res.* 123, 7678–7701 (2018).

***Flow in the deep troughs: A combination of barotropic and baroclinic flows³.
Barotropic flows are driven from the surface, baroclinic are driven by buoyancy forces***

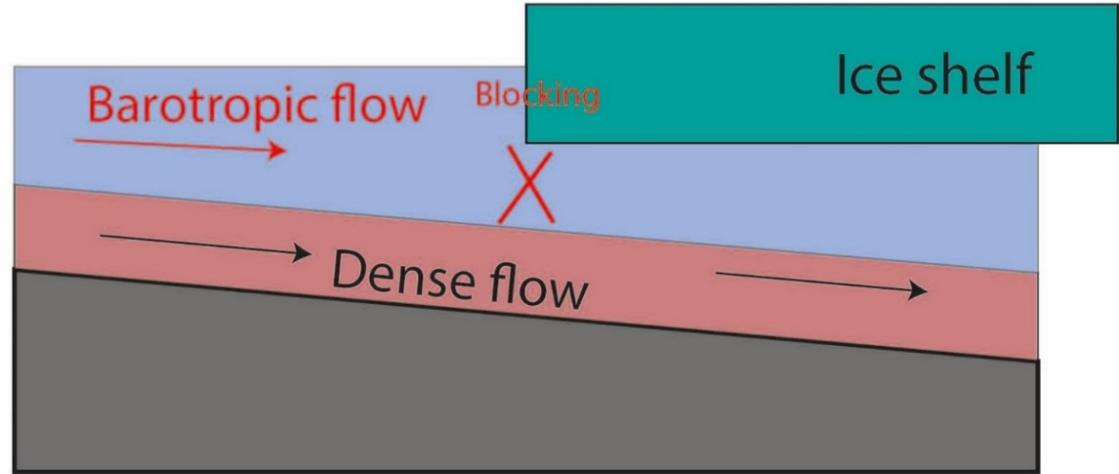
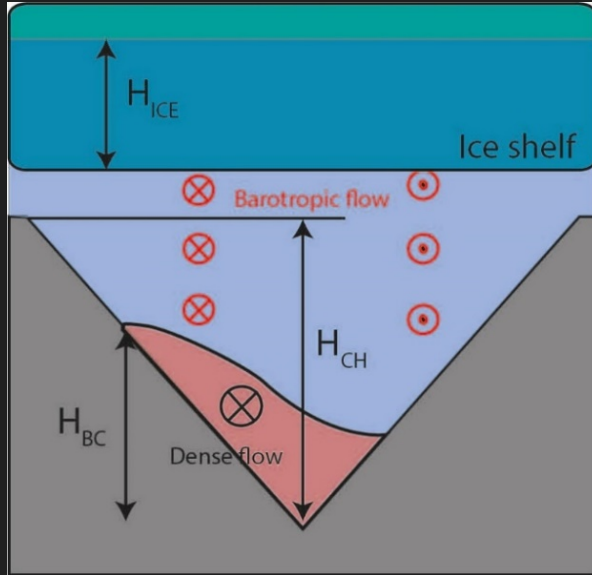
ADCP: Barotropic currents on Amundsen Shelf

Dense water leaning on bank, creating a baroclinic geostrophic dense current



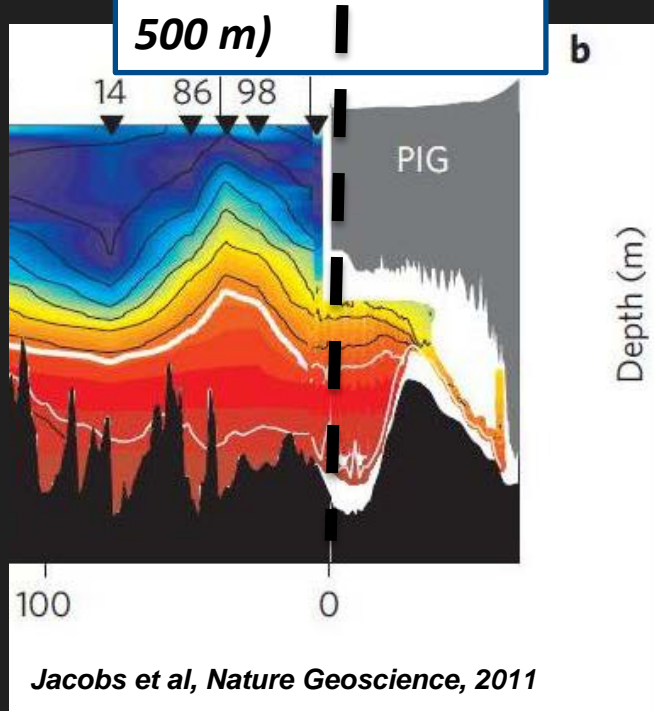
3) Kalén, O. et al: *Is the oceanic heat flux in the Amundsen Sea caused by barotropic or baroclinic currents...? Deep Sea Res. Part II Top. Stud. Oceanogr.* (2016) doi:10.1016/j.dsr2.2015.07.014

Simplified description of currents transporting heat to Antarctic ice shelves: Barotropic and baroclinic components

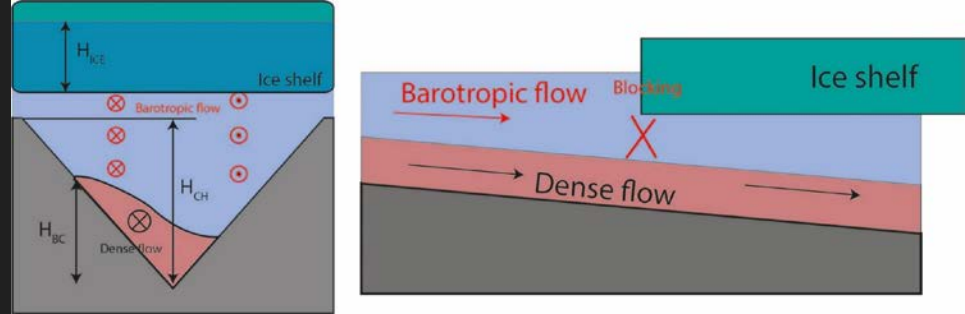


In order to access the floating ice shelves, the warm water has to get past the ice shelf front – a dramatic topographic barrier:

Ice shelf front (200-500 m)

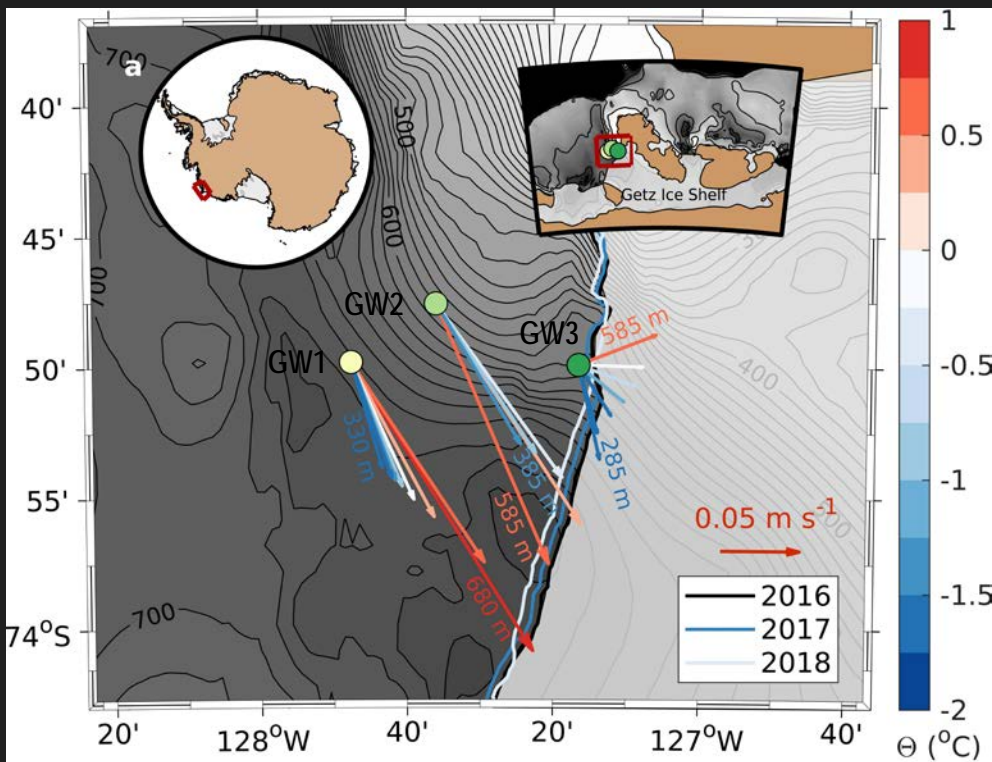


- Hypothesis: Blocks barotropic flow, but not baroclinic



Mooring data from Getz ice shelf front

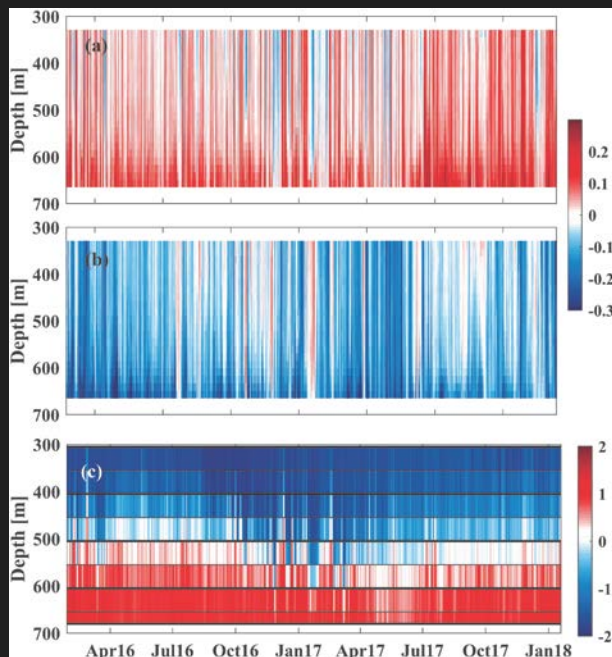
To examine the effect of the ice front on the along-trough current, three moorings equipped with velocity profilers and loggers for temperature, salinity, and pressure were placed in a deep trough leading to Getz Ice Shelf (left). Two of the moorings were positioned 14 km and 11 km away from the ice front at depths of 600 and 700 m respectively, while the third was placed 700-800 m from the front at 600 m depth. The ice front draft is 250-300 m, and its position was constant during the two years of measurements. Feather-plots of the average velocity at various depths for the three moorings show a persistent current up to 30 cm/s directed towards the ice shelf, parallel to the local bathymetry.



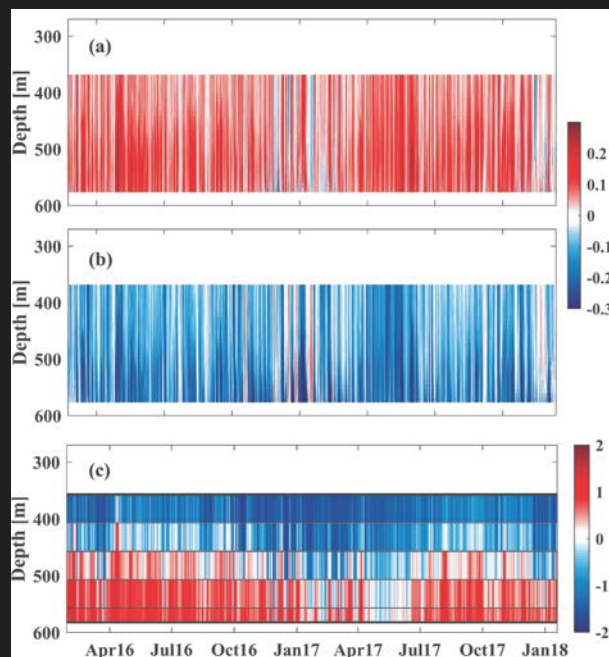
Velocity and temperature from the three moorings



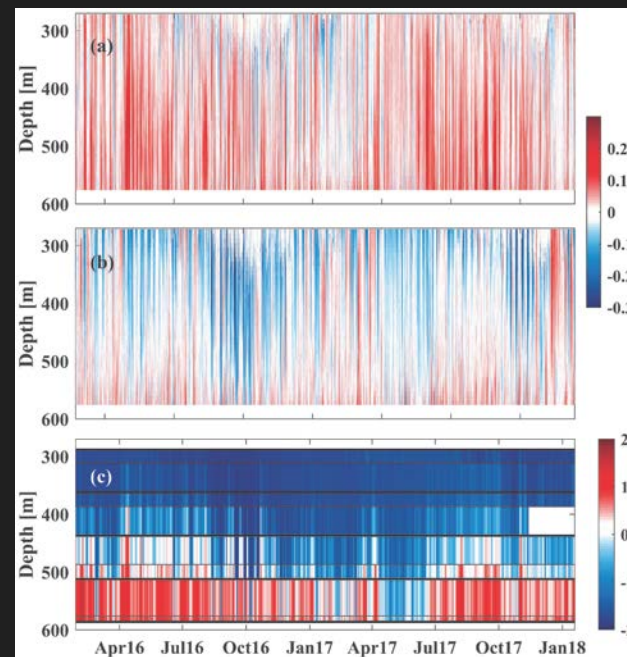
GW1 (safe distance)

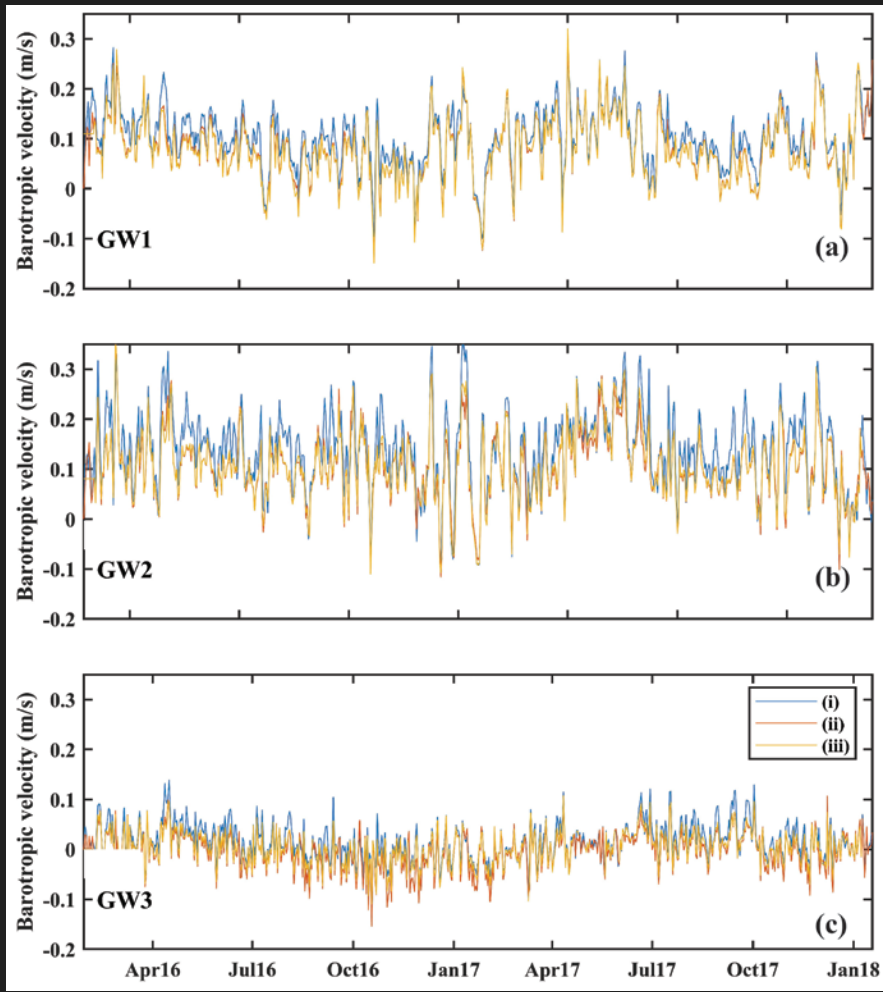


GW2 (safe distance)



GW3 (crazy distance)





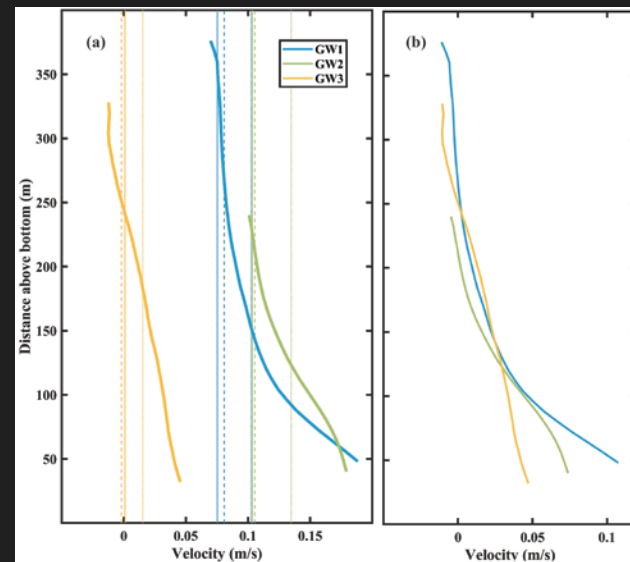
Barotropic and baroclinic velocity at the moorings

Separating the currents into barotropic and baroclinic components reveals that while GW1 and GW2 had significant barotropic along-slope flow (7.5 and 10 cm/s) with a baroclinic amplification in the warm bottom layer, the velocity at GW3 had a comparatively small barotropic component (0.1 cm/s) and was dominated by the baroclinic flow in the warm bottom layer. The direction of the baroclinic flow at GW3 is parallel to the local topography and orthogonal to the ice front.

Average velocity (solid)

Barotropic velocity (3 methods, thin lines)

Average baroclinic velocity



Correlation between the three moorings (Table 1)

	GW1: Bottom density	GW2: Bottom temperature	GW3: Bottom density	GW3: Velocity
GW2: Bottom temperature	0.62 (0.55)	-	-	-
GW3: Bottom density	0.67 (0.58)	0.92 (0.83)	-	-
GW1: Baroclinic velocity	0.54 (0.46)	0.71 (0.62)	0.77 (0.67)	0.66 (0.53)
GW1: Barotropic velocity	-0.09 (-0.03)	-0.08 (0.05)	-0.25 (-0.1)	-0.08 (0.02)
GW2: Baroclinic velocity	0.43 (0.36)	0.54 (0.49)	0.53 (0.45)	0.67 (0.51)
GW2: Barotropic velocity	0.15 (0.03)	0.20 (0.01)	0.09 (0.1)	0.23 (0.23)
GW3: Velocity	0.51 (0.36)	0.5 (0.39)	0.65 (0.57)	-

- High correlation between bottom temperature/density GW2 and GW3 => Flow at GW2 is strongly connected to flow at GW3
- Baroclinic velocity at both GW1 and GW2 strongly correlated to total velocity at GW3. Barotropic velocity uncorrelated => Barotropic velocity is blocked out, baroclinic continues to GW3

Heat flux induced by the two components

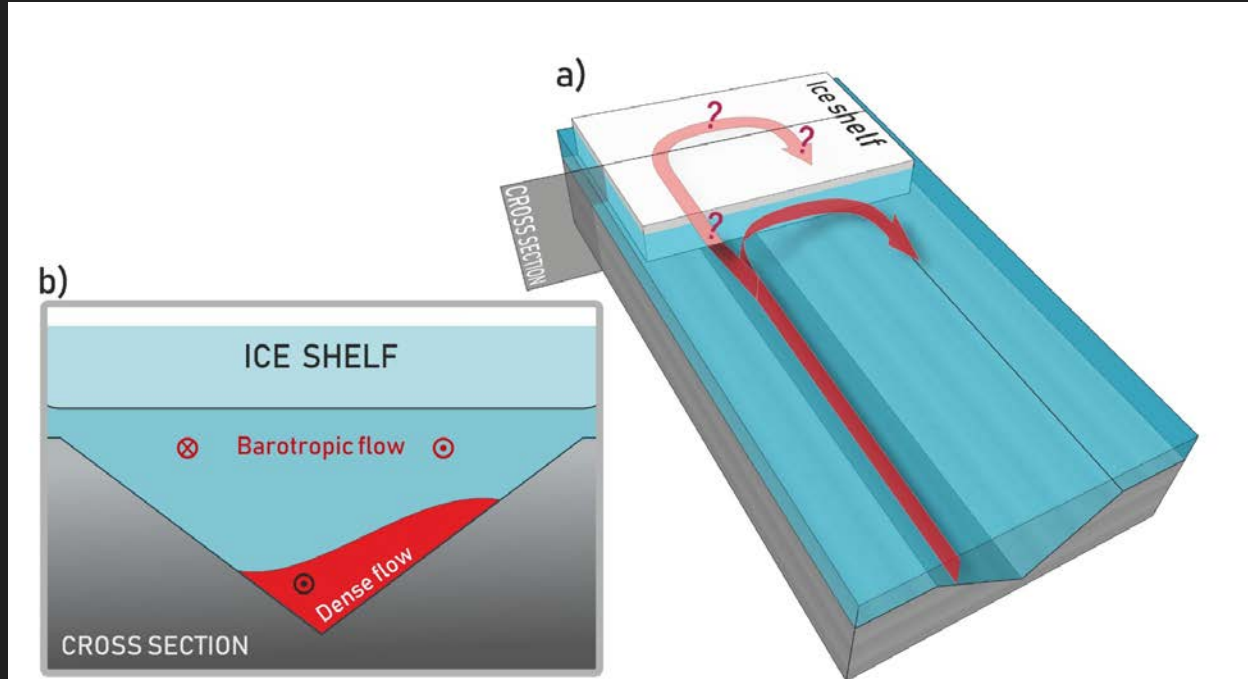
	GW1	GW2	GW3
H	2.8 TW	2.27 TW	0.47 TW
\bar{H}	2.64 TW (94%)	2.14 TW (94%)	0.38 TW (80%)
\tilde{H}	0.16 TW (6%)	0.13 TW (6%)	0.09 TW (20%)
H_{BT} (method (i))	2.49 TW (89%)	2.11 TW (93%)	0.28 TW (60%)
H_{BC} (method (i))	0.31 TW (11%)	0.16 TW (7%)	0.19 TW (40%)
H_{BT} (method (ii))	1.96 TW (70%)	1.61 TW (71%)	0.01 TW (3%)
H_{BC} (method (ii))	0.84 TW (30%)	0.66 TW (29%)	0.46 TW (97%)
H_{BT} (method (iii))	1.88 TW (67%)	1.59 TW (70%)	0.05 TW (10%)
H_{BC} (method (iii))	0.92 TW (33%)	0.68 TW (30%)	0.42 TW (90%)

Barotropic

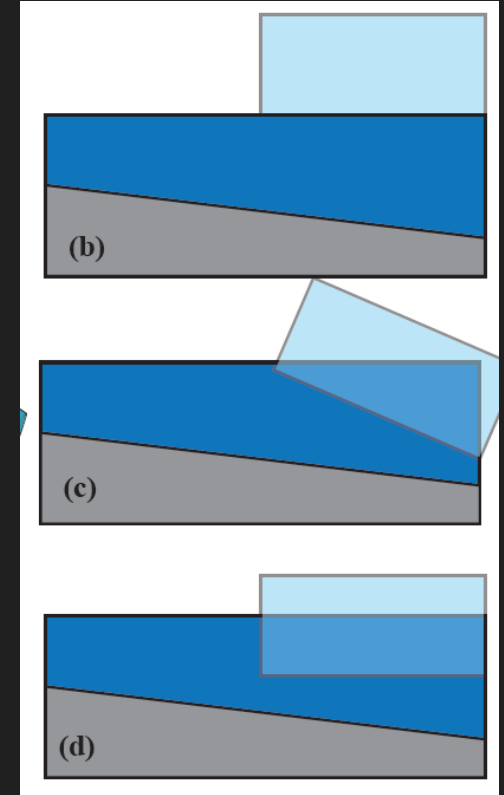
Baroclinic

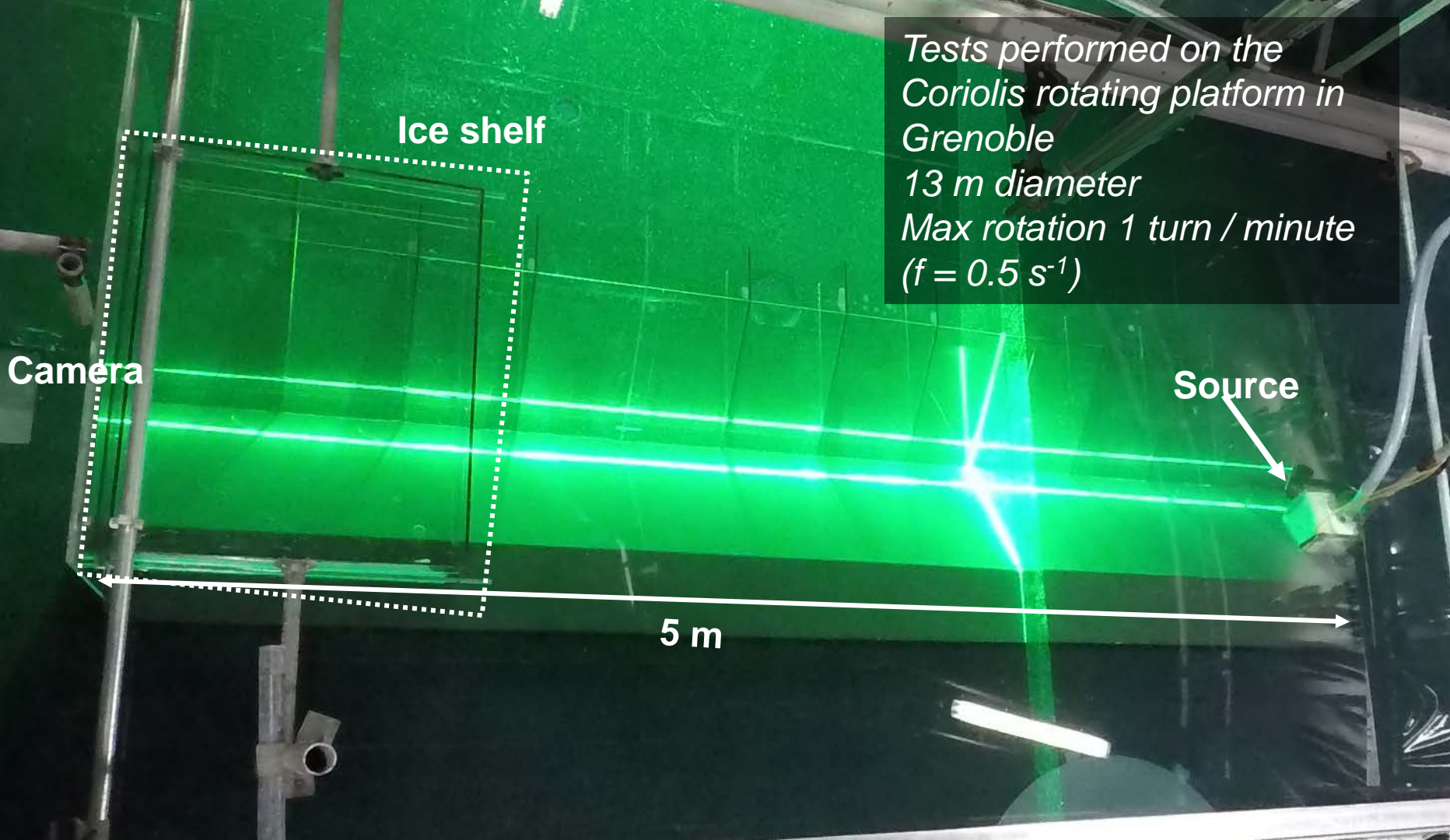
Barotropic heat flux component constitutes between 67% and 93% of the total heat flux at GW1 and GW2. At GW3 the barotropic component only makes up 3% - 40%, with the majority of the heat flux induced by the baroclinic component

Laboratory experiment



Three different ice shelves:





Tests performed on the
Coriolis rotating platform in
Grenoble
13 m diameter
Max rotation 1 turn / minute
($f = 0.5 \text{ s}^{-1}$)

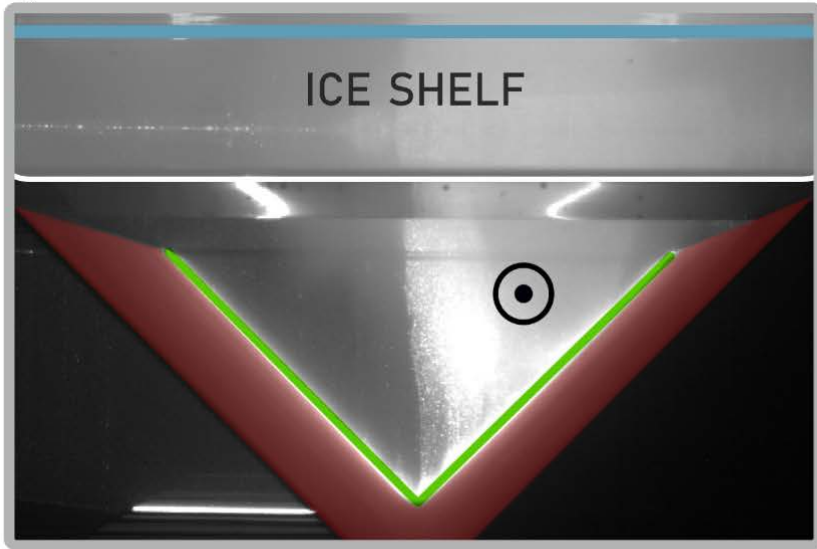
Ice shelf

Camera

Source

5 m

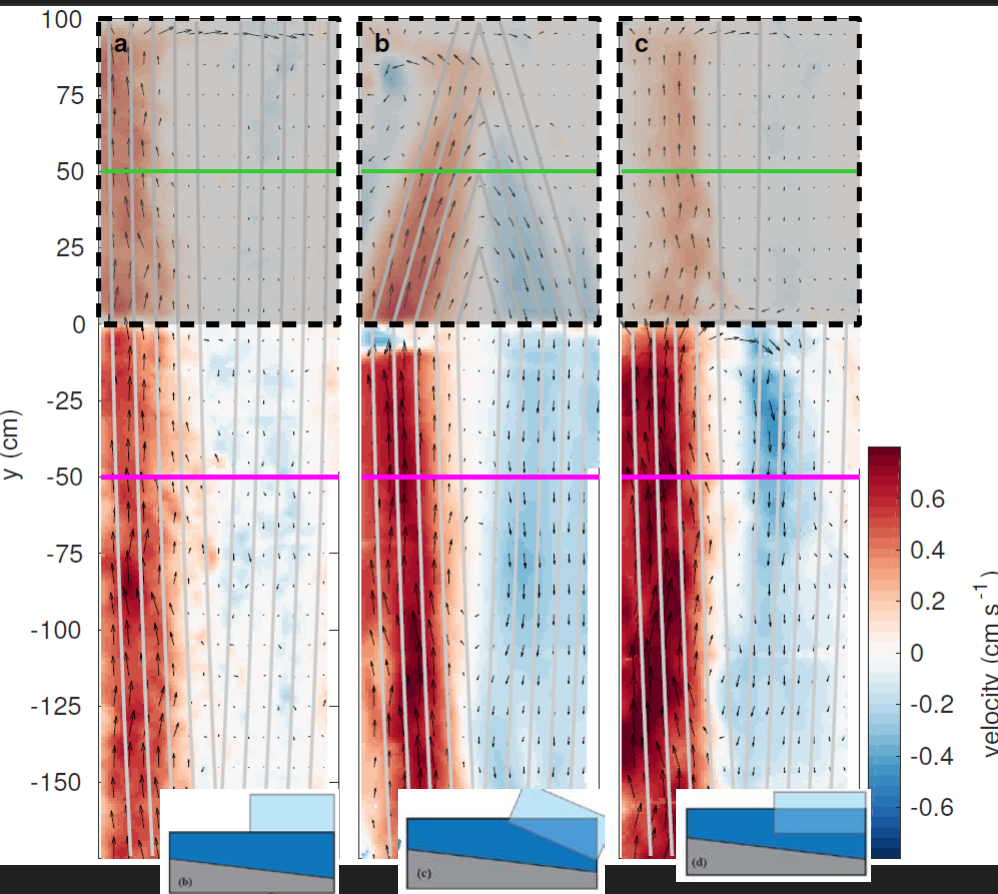
Barotropic



Baroclinic



Top view

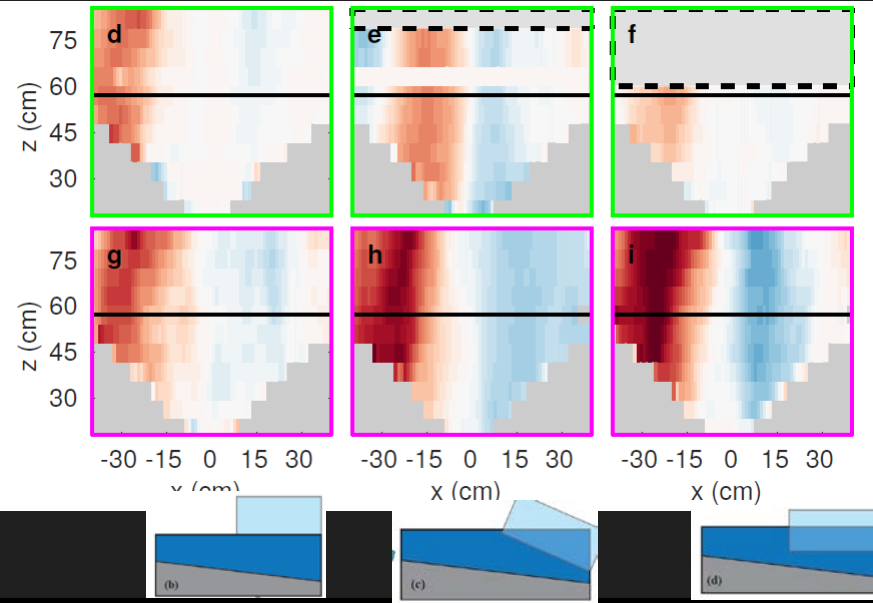


Barotropic flow

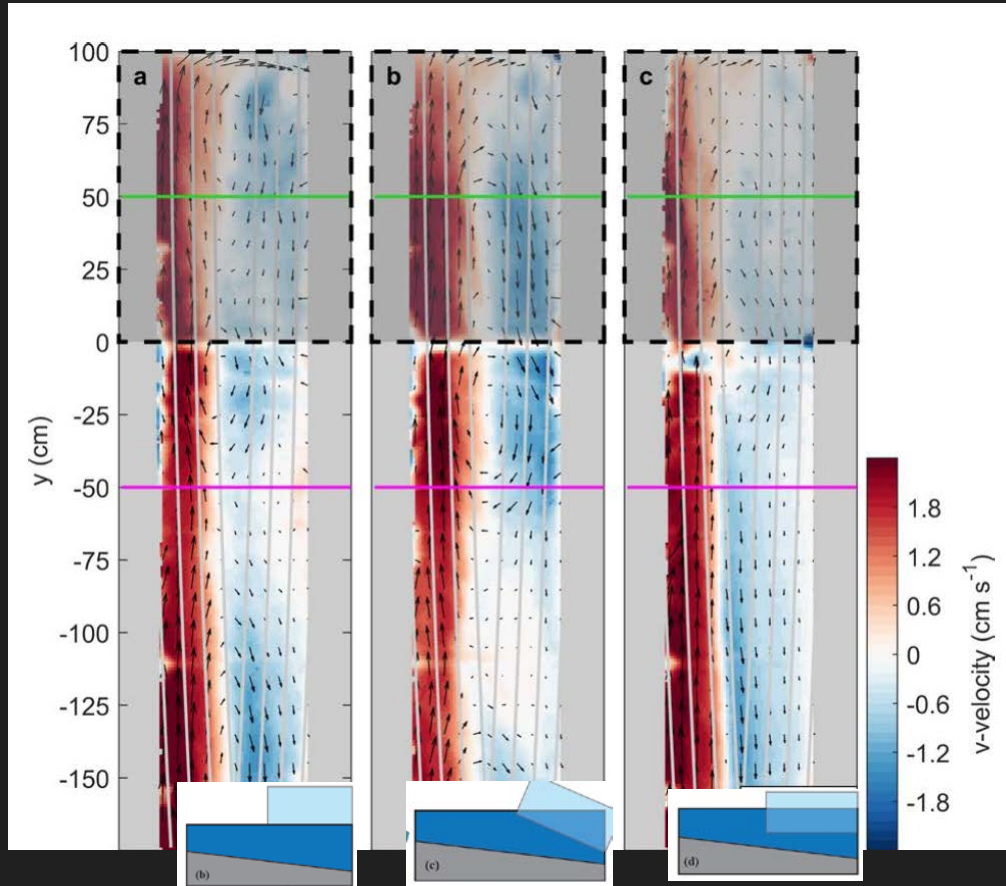
Stream lines parallel to water column thickness (gray lines)

Flow partly blocked for step-shaped ice shelf front

Side view



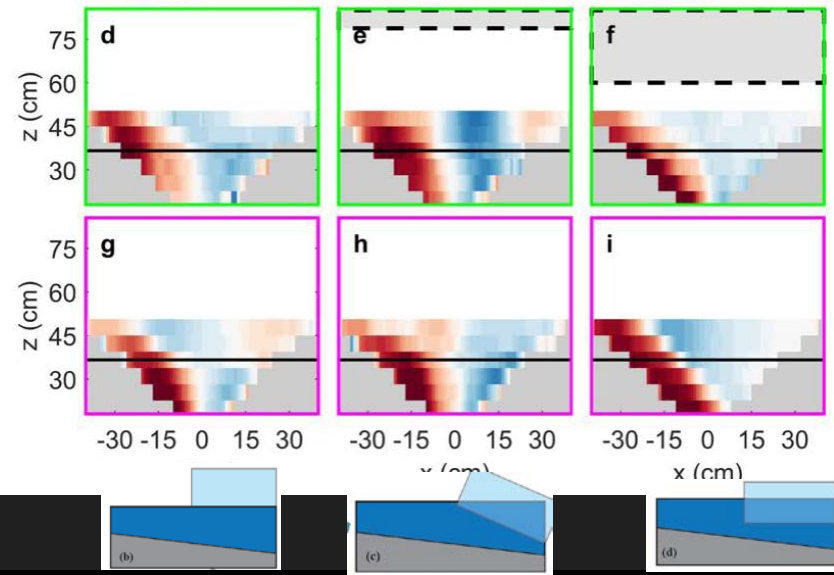
Top view



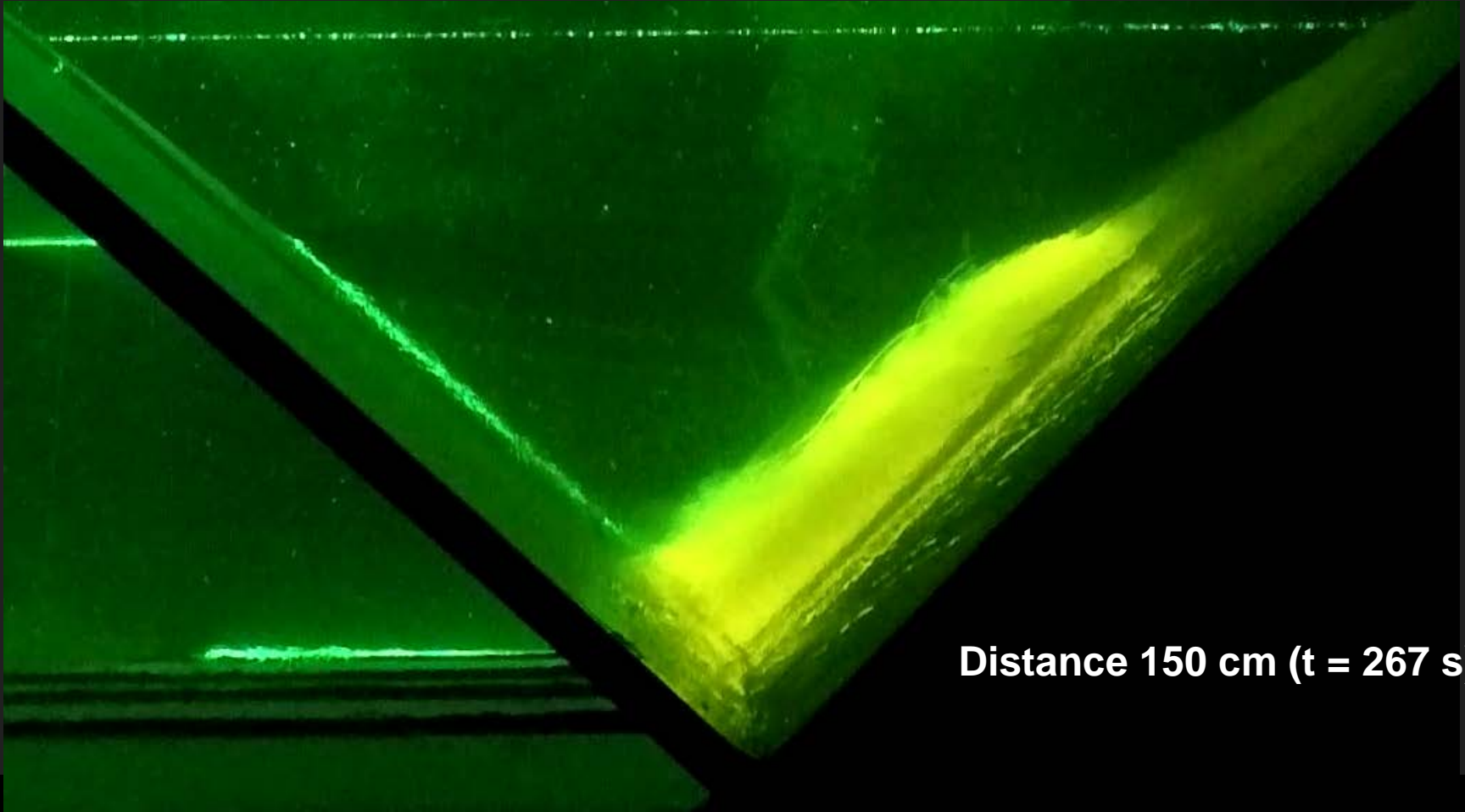
Baroclinic flow

Stream lines parallel to bathymetry (gray lines)
Flow not blocked or redirected for any shape
ice shelf front

Side view

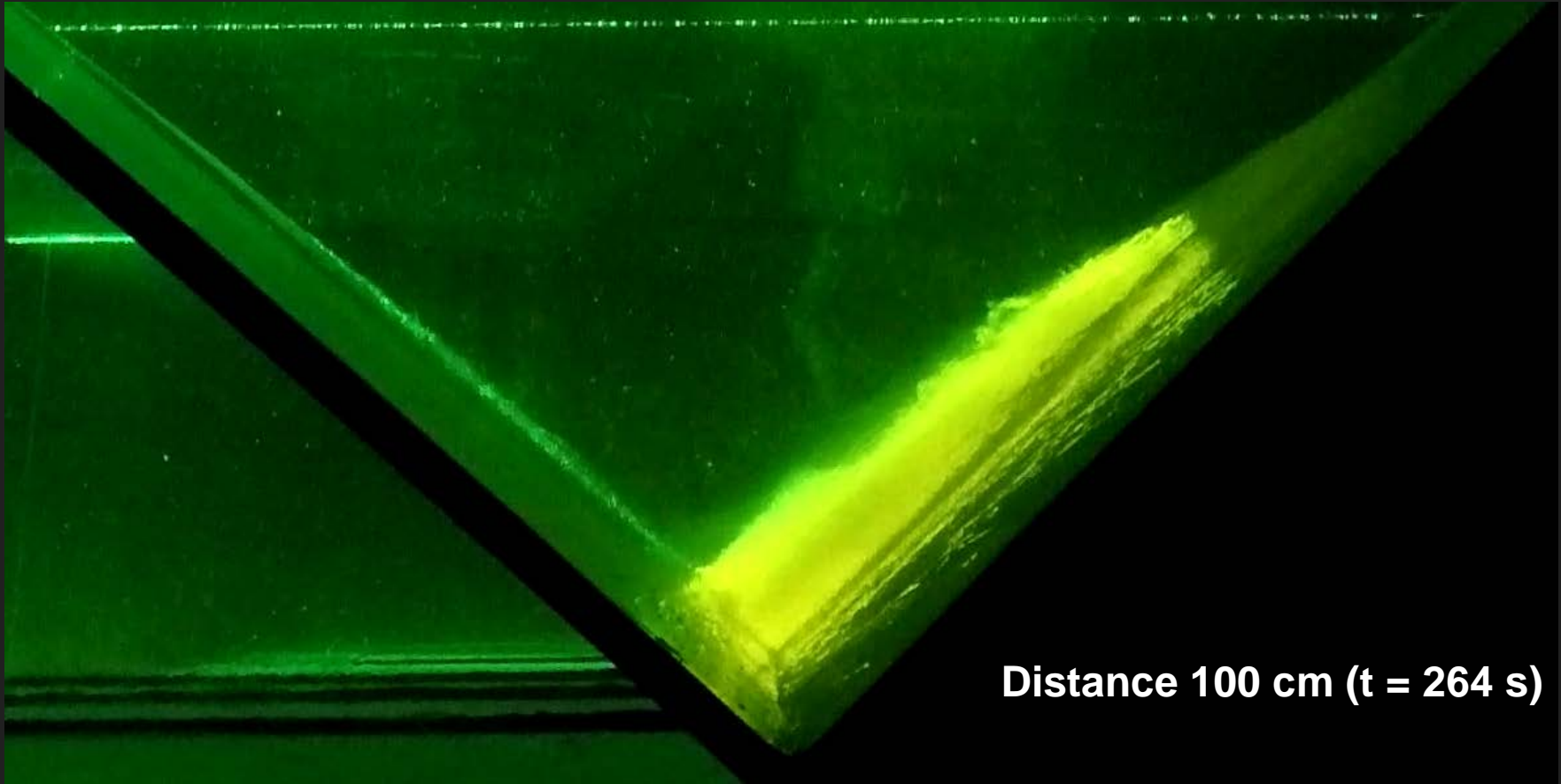


Cross section upstream channel (baroclinic flow)



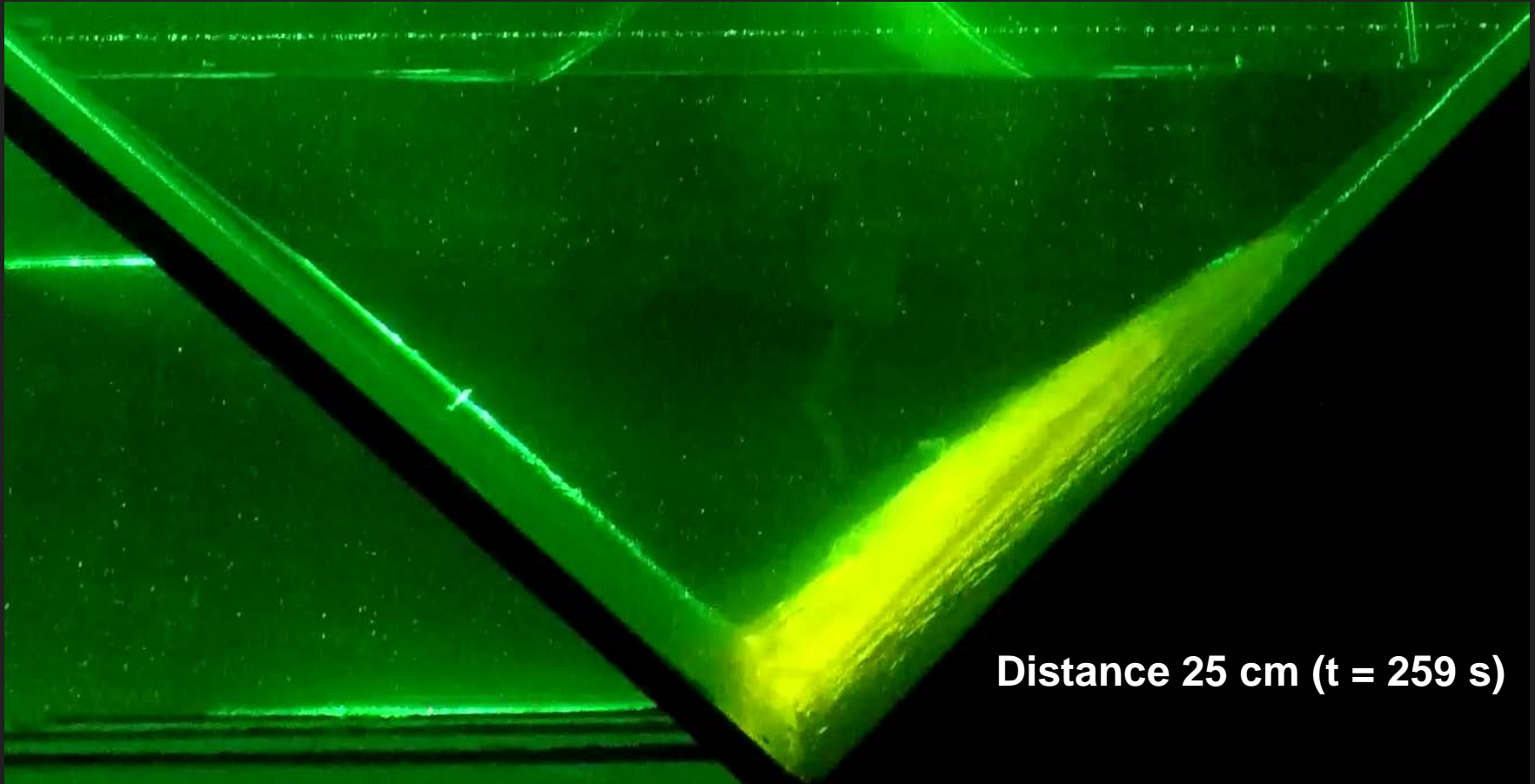
Distance 150 cm ($t = 267$ s)

Cross section upstream channel (baroclinic flow)



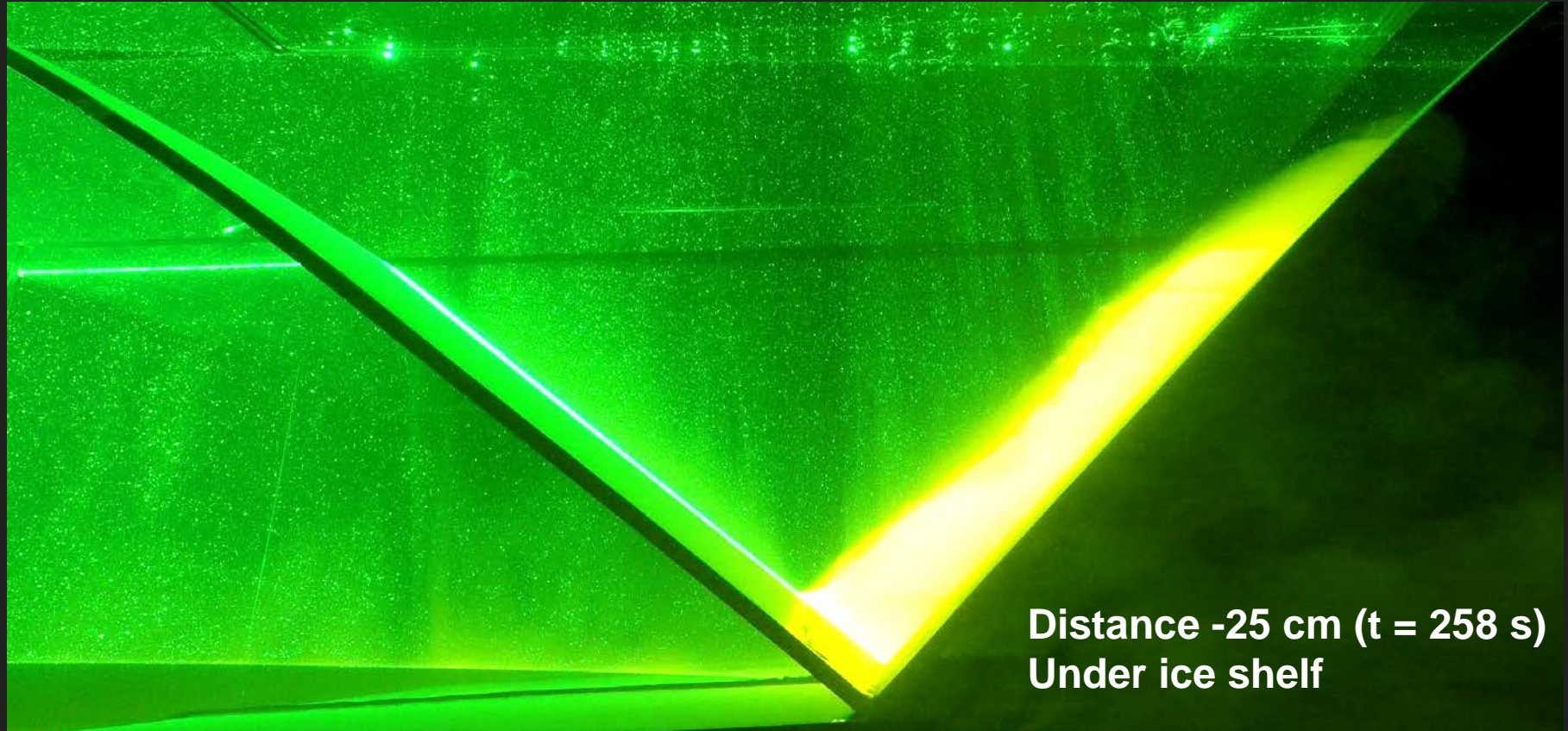
Distance 100 cm ($t = 264$ s)

Cross section upstream channel (baroclinic flow)



Distance 25 cm ($t = 259$ s)

Cross section under ice shelf (baroclinic flow)



Distance -25 cm ($t = 258$ s)
Under ice shelf

Thanks for reading!

Thanks to the Hydralab programme, the LEGI Coriolis facility
RVIB Araon

Swedish Research Council

SSF

Norwegian Research Council

Questions in chat or to anna@gu.se

